

文章编号: 1006-9941 (2016)06-0604-05

Structure and Formation Mechanism of Impurity in Nano-TATB

WANG Yan-qun¹, WANG Jun², HUANG Hui-sheng³, QIAO Zhi-qiang², LI Rui², SHEN Jin-peng², YANG Guang-cheng²

(1. School of Materials Science and Engineering, Southwest University of Science and Technology, Mianyang 621010, China; 2. Institute of Chemical Materials, China Academy of Engineering Physics, Mianyang 621999, China; 3. Chongqing Key Laboratory of Inorganic Special Functional Materials, Yangtze Normal University, Chongqing 408100, China)

Abstract: Nano-TATB (1, 3, 5-triamino-2, 4, 6-trinitrobenzene) is an insensitive high explosive (IHE), some impurities in its preparation process were produced. In this work, the structures of the impurities were studied by liquid-state ¹³C nuclear magnetic resonance spectroscopy, X-ray photoelectron spectroscopy and theoretical simulation method. Results show that the impurity is the proton compound of TATB molecule and it is named as 1, 3, 5-triamino-2, 4, 6-trinitro-2, 5-cyclohexadiene bisulfate. According to the quantum chemical method, the possible formation mechanism of this kind of impurity is the protonation of TATB molecule by H atom in concentrated H₂SO₄ during the dissolution process.

Key words: nano-TATB; impurity; proto compound; mechanism**CLC number:** TJ55; O64**Document code:** A**DOI:** 10.11943/j.issn.1006-9941.2016.06.016

1 Introduction

Among the various insensitive high explosives, 1, 3, 5-triamino-2, 4, 6-trinitrobenzene, commonly known as TATB, is an attractive insensitive explosive as it satisfies the safety requirements at high temperatures and its resistance to accidental initiation and explosion^[1-2]. Compared with raw TATB, nano-TATB has more potential applications due to higher sensitivity to short-duration pulse shock initiation, higher stability and higher detonation velocity^[3]. For military, nano-TATB is used in modern nuclear warheads^[4], slapper detonation^[5]. Nano-TATB is also used as an insensitive coating surface to reduce the mechanical sensitivity of HMX (1, 3, 5, 7-tetranitro-1, 3, 5, 7-tetrazocane)^[6] or CL-20 (2, 4, 6, 8, 10, 12-hexanitro-2, 4, 6, 8, 10, 12-hexaazaisowurtzitane)^[7] and to enhance the mechanical performance of PBX (polymer bonded explosive)^[8]. Moreover, nano-TATB is used in deep oil well explorations in the civilian community, and as a reagent in the manufacture of liquid crystal displays. Therefore, the preparation of nano-TATB is an important issue because of its wide applications. According to literatures^[5, 9], solvent/non-solvent recrystallization is one of the most effective method to prepare nano-TATB. However, TATB molecule has strong hydrogen bonds that induce a strong dipole-dipole van der Waals-Keesom force and results in low solubility in most of the organic solvents^[1]. Concentrated H₂SO₄ is good solvent of TATB molecule to prepare nano-TATB particles because of high solubility of TATB in concentrated H₂SO₄. In our previous report^[5], nano-TATB particles with an average diameter of 60 nm were firstly pre-

pared by using solvent/non-solvent recrystallization method with concentrated H₂SO₄ as solvent and water as non-solvent. Moreover, this approach achieves the large-scale preparation of the products. Yang et al^[3] further studied the influencing factors of this method on the grain size and crystal morphology of nano-TATB. Results indicated that the obtained nano-TATB had even grain size and good uniformity by adding the surfactants and changing the volume ratio of solvent to non-solvent. Liu et al^[10] investigated the nano-scale effects of TATB on thermal decomposition kinetics through dynamic vacuum stability test and the results revealed that the nanoparticles (NPs) show much higher reaction activity than the micro particles (MPs). According to our researches, there are some impurity in nano-TATB prepared by concentrated H₂SO₄ as solvent and water as non-solvent. The impurity may be the residual H₂SO₄, and the protonation or solvation compounds of TATB molecule because of strong oxidizing of concentrated H₂SO₄. Large amounts of impurities would adversely affect the long-term storage, energetic properties and safety. However, there are no literatures studied on impurity in nano-TATB prepared by concentrated H₂SO₄ as solvent and water as non-solvent.

In this work, we present both experimental characterization and theoretical simulation methods to investigate the structure and formation mechanism of impurity in nano-TATB prepared by concentrated H₂SO₄ as solvent and water as non-solvent. The structure of the impurity was confirmed by using liquid-state ¹³C-NMR and theoretical simulation techniques. Theoretical calculation method was used to evaluate their relative stabilities and calculate ¹³C-NMR chemical shifts of possible impurities. XPS was carried out to further identify the impurity in nano-TATB sample. Moreover, the possible formation mechanism of impurity in nano-TATB prepared by concentrated H₂SO₄ as solvent was investigated depending on the quantum chemical method.

2 Experimental

2.1 Preparation of Nano-TATB with Different Purity

Nano-TATB was prepared by solvent/non-solvent recryst-

Received Date: 2015-11-03; **Revised Date:** 2015-12-03**Project Supported:** National Natural Science Foundation of China (11272292, 11372288) National High Technology Research and Development Program of China (863Program) (2013AA050905) and the Chunhui Program of Ministry of Education of China (Z2014084). Development Foundation of CAEP (2014B0302041), and Young Talent Foundation of Institute of Chemical Materials (KJZX-201403).**Biography:** WANG Yan-qun (1991-), female, master, research field: preparation of high purity nano-TATB. e-mail: 15228356303@163.com**Corresponding Author:** YANG Guang-cheng (1976-), male, professor, research field: preparation of nano explosive. e-mail: ygcheng@caep.cn

tallization method with concentrated H_2SO_4 as solvent and ultra-pure water as non-solvent^[5]. Raw TATB was dissolved in concentrated H_2SO_4 . Then, the solution and some ultra-pure water were added into the sprayed instrument. Through rapid crystallization, washing and vacuum freeze-drying, nano-TATB particles were obtained. Nano-TATB with different purity was prepared by varying the experimental conditions.

2.2 Characterization

2.2.1 Computational Method

The three-dimensional structures of all the studied compounds were built using the GaussView program. Equilibrium geometries, harmonic vibrational frequencies, and ^{13}C NMR chemical shifts were calculated using the B3LYP functional with the 6-31+G** basis set. Chemical shifts were computed employing the gauge including atomic orbital (GIAO) method^[11-12], with tetramethylsilane (TMS) as an internal reference. Formation mechanism of the impurity in nano-TATB was investigated at the B3LYP/6-31+G** level. The geometries of reactants, transition state and product were optimized. Vibration analysis was performed to verify whether each species was a minimum or a transition state on the potential energy surface. The pathway between the transition state and its connected minima was confirmed by the intrinsic reaction coordinate (IRC) calculation^[13-14]. All density functional theory calculations reported in this work were carried out with the Gaussian 03 software package.

2.2.2 Characterization of Nano-TATB with Different Purity

The liquid-state ^{13}C NMR spectrum was recorded on a Bruker Avance III 600 spectrometer. The solution was obtained by dissolving 100 mg of raw TATB in 0.6 mL of concentrated H_2SO_4 , with D_2O as external standard. X-ray photoelectron spectroscopy (XPS) study was performed using an ESCALAB 250 XPS X-ray Electron Spectrometer (American Thermo Electron Corporation). Sulfur content was detected by microcoulometry.

3 Results and Discussion

3.1 Identification of the Structure of the Impurity

There are some impurities in nano-TATB prepared by concentrated H_2SO_4 as solvent and water as non-solvent. The impurity may be the residual H_2SO_4 or the protonation or solvation compounds of TATB molecule because of strong oxidizing of concentrated H_2SO_4 . Firstly, the sulfur content in nano-TATB with different purity was measured using microcoulometry. The corresponding H_2SO_4 content is given by the following equation:

$$Y = \frac{M_1 X}{M_2 100} = \frac{98 X}{32 100}$$

Where, M_1 is the molecular mass of H_2SO_4 ($\text{g} \cdot \text{mol}^{-1}$), M_2 is the molecular mass of sulfur ($\text{g} \cdot \text{mol}^{-1}$), X is the sulfur content and Y is the H_2SO_4 content.

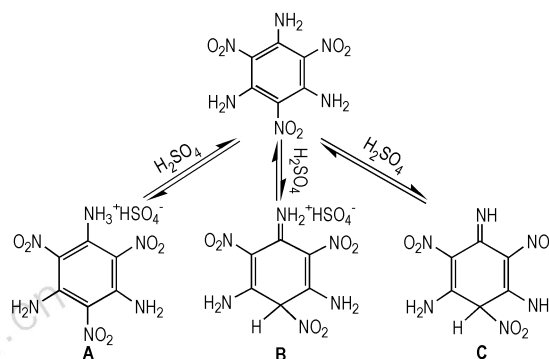
The results are listed in Table 1. The calculated residual H_2SO_4 content in nano-TATB with purity of 89%, 95%, and 96% are approximately 0.2223%, 0.165%, 0.098%, respectively. While the total impurity content in nano-TATB are

11%, 5% and 4%, respectively. The results indicate that the impurity content is much higher than the residual H_2SO_4 content. To our knowledge, during the recrystallization process of nano-TATB, the suspension containing nano-TATB colloid particles was washed with water to remove residuary acid until the pH value reached 6-7. Therefore, the existence of the residual H_2SO_4 in nano-TATB is impossible. The impurity in nano-TATB should be the protonation or solvation compound of TATB.

Table 1 Total sulfur, H_2SO_4 , and impurity content in nano-TATB with different purity

purity of nano-TATB/%	89	95	96
sample mass/mg	100.6	100.6	100.6
total sulfur/%	0.0726	0.0540	0.0320
H_2SO_4 content/%	0.2223	0.165	0.098
impurity content/%	11	5	4

Earlier Harris^[15] suggested that there were three possible protonated or solvated compounds of TATB, after TATB was dissolved in concentrated H_2SO_4 . The possible structures were presented in Scheme 1. The structure A was obtained from the protonation effect at the amino group and solvation effect at the TATB ring. Differently, the structure B was produced from the protonation and solvation effect both at the TATB rings, while the structure C formed only from the solvation effect of TATB.



Scheme 1

In order to verify the most possible structure form of TATB in concentrated H_2SO_4 , we compared the structure stability and simulated the liquid state ^{13}C NMR of above three possible structures.

3.1.1 The Oretical Simulation of Three Possible Structures

In order to confirm possible impurity (protonation or solvation compound of TATB molecule) in nano-TATB, the stabilities of isoelectronic systems of the three possible structures shown in Scheme 1 are systematically investigated. As shown in Table 2, A^+ and B^+ represent the cations of compound A and B shown in Scheme 1, respectively. The optimized geometry, total energy and energy gap between the highest occupied molecular orbital (HOMO) and the lowest unoccupied molecular orbital (LUMO) are given in Table 2. The results show that the total energy decreases in the order of $\text{C} > \text{A}^+ > \text{B}^+$ and the energy gap decreases in the following sequence: $\text{B}^+ >$

$A^+ = C$. Therefore, B^+ is more stable than A^+ and C . The results reveal that compound B exhibits better stability and is the most possible protonation compound of TATB molecule in concentrated H_2SO_4 .

Table 2 Calculated results of the related compounds by B3LYP method

compound	A^+	B^+	C
geometric structure			
total energy /Hartree	-1012.212284	-1012.218912	-1011.826964
energy gap/eV	3.55	4.10	3.55

In addition, the calculated ^{13}C chemical shifts of compounds A , B , and C shown in Scheme 1 and the experimental liquid-state ^{13}C NMR of TATB in concentrated H_2SO_4 are displayed in Fig. 1. The measured ^{13}C chemical shifts of TATB in concentrated H_2SO_4 are 154.54, 151.66, 150.29, 113.27, and 83.68 (see Fig. 1). In comparison with the calculated ^{13}C chemical shifts of compounds A , B , and C , the computed NMR signals of compound B are in best agreement with the experimental data. The results further reveal that compound B is the most possible protonation compound of TATB molecule in concentrated H_2SO_4 . Thus, based on the above theory simulation and liquid-state ^{13}C NMR results, we can conclude that the protonation compound of TATB molecule in concentrated H_2SO_4 is compound B shown in Scheme 1, and the corresponding structure was characterized as 1,3,5-triamino-2,4,6-trinitro-2,5-cyclohexadien bisulfate.

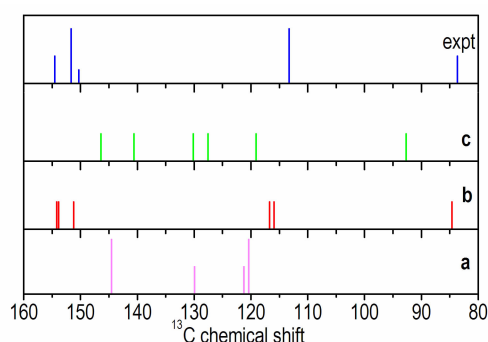
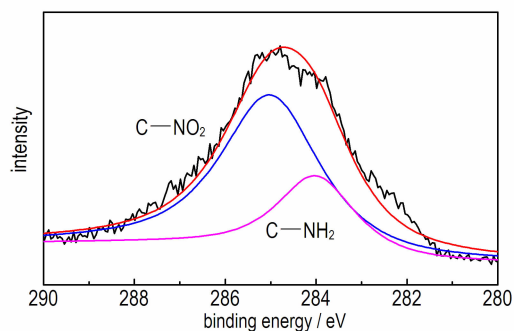


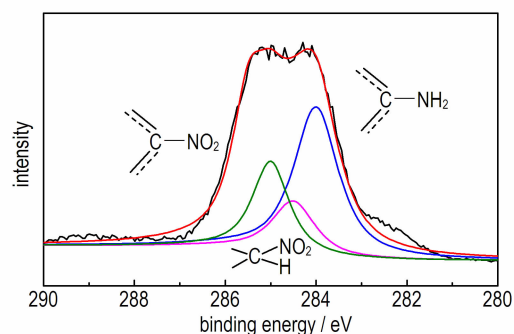
Fig. 1 Comparison of the calculated and experimental ^{13}C NMR chemical shifts (a, b and c represent the calculated liquid-state ^{13}C NMR of compounds A , B , C shown in Scheme 1, respectively)

Nano-TATB preparation involves two main processes: dissolution and recrystallization. Firstly, raw TATB was dissolved into concentrated H_2SO_4 . After complete dissolution, the solution recrystallized in water to obtain yellow nano-TATB particles. In order to further confirm the impurity in nano-TATB sample, the nano-TATB with different purity was measured XPS characterization. It is well known that XPS is a very useful technology to determinate chemical composition and functional groups of samples.

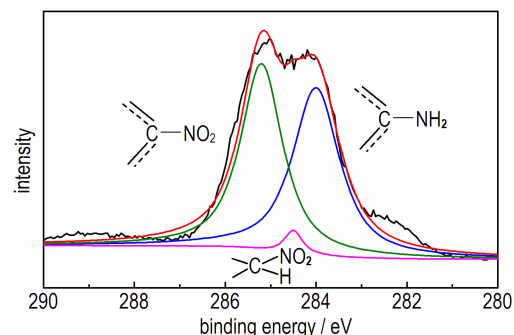
Figure 2 shows the $C1s$ XPS spectra of raw TATB with purity of 99.9% and nano-TATB with purity of 89%, 95%, and 96%. XPS spectra of raw TATB and nano-TATB with different purity are compared to investigate major differences in functional groups. The peaks at 284 eV and 285 eV are assigned to $-NH_2$ and $-NO_2$ groups, respectively, (Fig. 2a). However, the curve fitting of $C1s$ peaks of nano-TATB with different



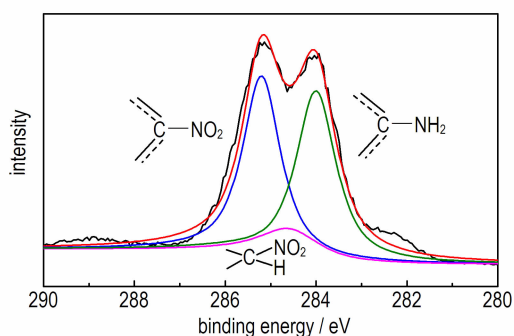
a. raw TATB



b. nano-TATB with purity of 89%



c. nano-TATB with purity of 95%



d. nano-TATB with purity of 96%

Fig. 2 Curves fitting of $C1s$ peaks of the XPS spectra of different samples

purity (Figs. 2b, 2c, 2d) shows the existence of three different groups: $-\text{NH}_2$, $-\text{NO}_2$ and $-\text{CH}(\text{NO}_2)$ groups. By comparing the experimental results obtained with XPS, it can be concluded that impurity (compound B, 1,3,5-triamino-2,4,6-trinitro-2,5-cyclohexadien bisulfate) was formed in nano-TATB due to the existence of $-\text{CH}(\text{NO}_2)$ group. Moreover, the peak area of $-\text{CH}(\text{NO}_2)$ groups reduces as the increase of the impurity content, it further indicates that the impurity is 1,3,5-triamino-2,4,6-trinitro-2,5-cyclohexadien bisulfate.

3.2 Formation Mechanism of 1,3,5-Triamino-2,4,6-trinitro-2,5-cyclohexadien Bisulfate

TATB is a planemolecule and has strong inter- and intramolecular hydrogen bonds. Upon TATB dissolution, the symmetry and hydrogen bond were destroyed by concentrated H_2SO_4 . The reaction mechanism of TATB and concentrated H_2SO_4 to form protonation compound 1,3,5-triamino-2,4,6-trinitro-2,5-cyclohexadien bisulfate was analyzed by using the quantum chemistry method. The corresponding optimized geometries of the reactants, product, and transition state are depicted in Fig. 3. The reaction between TATB and concentrated H_2SO_4 consists of one step and one transition state is formed. As shown in Fig. 3, when TATB dissolved in concentrated H_2SO_4 and reacted, the bond length of $\text{C}(1)-\text{N}(1)$ of TATB molecule increases from 1.432 Å to 1.520 Å, whereas the bond length of $\text{S}(1)-\text{O}(1)$ of H_2SO_4 molecule decreases from 1.616 Å to 1.548 Å. The bond angle of $\angle\text{S}(1)-\text{O}(1)-\text{H}(1)$ of H_2SO_4 molecule varies from 109.8° to 113.5°, and the $\angle\text{C}(2)-\text{C}(1)-\text{C}(3)$ of TATB molecule decreases from 121.0° to 119.1°. The $\text{H}(1)$ proton of H_2SO_4 molecule moves closer to the $\text{C}(1)$ atom of TATB molecule, resulted in the $\text{O}(1)-\text{H}(1)$ bond of TATB molecule is weakened, and the transition state is formed (Fig. 3 TS). The TS structure, the bond angle $\angle\text{O}(1)-\text{H}(1)-\text{C}(1)$ of the transition state TS structure is 176.1°. After that, the $\text{C}(1)$ atom of TATB molecule is attacked by the $\text{H}(1)$ proton of H_2SO_4 molecule. In this process, the bond length of $\text{C}(1)-\text{H}(1)$ of TATB molecule decreases from 1.344 Å to 1.098 Å, whereas that of $\text{O}(1)-\text{H}(1)$ of TATB molecule increases from 1.258 Å

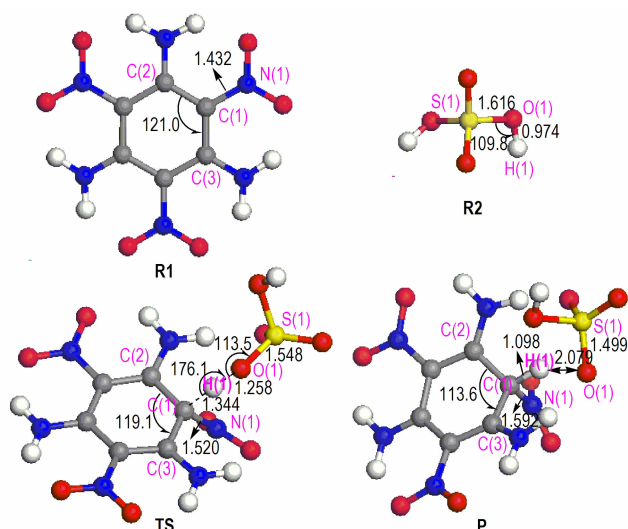


Fig. 3 Geometric parameters of reactants (R1 and R2), transition state (TS), and product (P) (bond length in Å, bond angle in degree)

to 2.079 Å. Therefore, the $\text{O}(1)-\text{H}(1)$ bond of concentrated H_2SO_4 molecule is broken and $\text{H}(1)$ is detached, resulting in the formation of 1,3,5-triamino-2,4,6-trinitro-2,5-cyclohexadien bisulfate.

Moreover, the diagram of the relative energies along the channel of the reaction is presented in Fig. 4. It shows that the reaction is an endothermic process. For the $\text{R1}+\text{R2}\rightarrow\text{TS}$, the activation energy of transition state TS reacted by TATB and H_2SO_4 is $46.1\text{ kJ}\cdot\text{mol}^{-1}$ and the heat of reaction is about $6.6\text{ kJ}\cdot\text{mol}^{-1}$. The results show that the formation process of 1,3,5-triamino-2,4,6-trinitro-2,5-cyclohexadien bisulfate easily occurs without heating or catalysts. The reaction is completed only through a transition state without an intermediate.

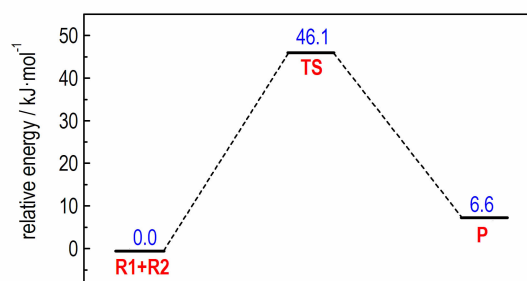


Fig. 4 Diagram of relative energies along the channel of the reaction

4 Conclusions

The impurity in nano-TATB prepared by concentrated H_2SO_4 as solvent and deionized water as non-solvent was successfully demonstrated to be a protonation compound of TATB molecule by concentrated H_2SO_4 . The structure is characterized as 1,3,5-triamino-2,4,6-trinitro-2,5-cyclohexadien bisulfate. According to the quantum chemical method, the impurity is easily formed in concentrated H_2SO_4 because of the activation energy of transition state is $46.1\text{ kJ}\cdot\text{mol}^{-1}$ and the heat of reaction is about $6.6\text{ kJ}\cdot\text{mol}^{-1}$. These results will provide useful reference information for the preparation of high purity nano-TATB and improvement of performance on nano-TATB.

References:

- [1] Boddu V M, Viswanath D S, Ghosh T K, et al. 2,4,6-triamino-1,3,5-trinitrobenzene (TATB) and TATB-based formulations-a review[J]. *Journal of Hazardous Materials*, 2010, 181(1): 1-8.
- [2] LIU Hong, ZHAO Ji-jin, JI Guang-fu, et al. Vibrational properties of molecule and crystal of TATB; A comparative density functional study[J]. *Physics Letters. A*, 2006, 358(1): 63-69.
- [3] YANG Li, REN Xiao-ting, LI Tie-cheng, et al. Preparation of ultrafine TATB and the technology for crystal morphology control [J]. *Chinese Journal of Chemistry*, 2012, 30(2): 293-298.
- [4] ZHANG Hao-bin, SUN Jie, KANG Bin, et al. Crystallmorphology controlling of TATB by high temperature anti-solvent recrystallization [J]. *Propellants, Explosives, Pyrotechnics*, 2012, 37(2): 172-178.
- [5] YANG Guang-cheng, NIE Fu-de, HUANG Hui, et al. Preparation and characterization of nano-TATB explosive [J]. *Propellants, Explosives, Pyrotechnics*, 2006, 31(5): 390-394.
- [6] MA Zhi-gang, GAO Bing, WU Peng, et al. Facile, and large-

- scale production of core-shell HMX@ TATB composites with superior mechanical properties by a spray-drying process[J]. *RSC Advances*, 2015, 5(27): 21042–21049.
- [7] YANG Zhi-jian, LI Jin-shan, HUANG Bin, et al. Preparation and properties study of core-shell CL-20/TATB composites[J]. *Propellants, Explosives, Pyrotechnics*, 2014, 39(1): 1–8.
- [8] LIN Cong-mei, LIU Shi-jun, HUANG Zhong, et al. The dependence of the non-linear creep properties for TATB-based polymer bonded explosives on the molecular structure of polymer binder[J]. *RSC Advances*, 2015, 5(39): 30592–30601.
- [9] TAN Xue-rong, DUAN Xiao-hui, PEI Chong-hua, et al. Preparation of nano-TATB by semibatch reaction crystallization[J]. *Nano: Brief Reports and Reviews*, 2013, 8(5): 1300551–1300558.
- [10] LIU Rui, YU Wei-fei, ZHANG Tong-lai, et al. Nanoscale effect on thermal decomposition kinetics of organic particles: dynamic vacuum stability test of 1,3,5-triamino-2,4,6-trinitrobenzene[J]. *Physical Chemistry Chemical Physics*, 2013, 15(20): 7889–7895.
- [11] Giesen D J, Zumbulyadis N. A hybrid quantum mechanical and empirical model for the prediction of isotropic ^{13}C shielding constants of organic molecules[J]. *Physical Chemistry Chemical Physics*, 2002, 4(22): 5498–5507.
- [12] Bagno A, Rastrelli F, Saielli G. Toward the complete prediction of the ^1H and ^{13}C NMR spectra of complex organic molecules by DFT methods: application to natural substances[J]. *Chemistry A European Journal*, 2006, 12(21): 5514–5525.
- [13] Head-Gordon M, Pople J A. A method for two-electron gaussian integral and integral derivative evaluation using recurrence relations[J]. *The Journal of Chemical Physics*, 1988, 89(9): 5777–5786.
- [14] Fukui K. The path of chemical reactions—the IRC approach[J]. *Accounts of Chemical Research*, 1981, 14(12): 363–368.
- [15] Harris B W. Carbon-13 NMR analyses of TATB and related compounds in sulfuric acid, LA-7572[R]. New Mexico, USA: Los Alamos Scientific Lab, 1979.

纳米 TATB 中杂质结构与形成机理

王彦群¹, 王 军², 黄辉胜³, 谯志强², 李 瑞², 沈金鹏², 杨光成²

(1. 西南科技大学材料科学与工程学院, 四川 绵阳 621010; 2. 中国工程物理研究院化工材料研究所, 四川 绵阳 621999; 3. 长江师范学院无机特种功能材料实验室, 重庆 408100)

摘要: 纳米 TATB 是一种高能钝感炸药, 在其制备过程中会产生一些杂质。采用液态 ^{13}C NMR、X 射线光电子能谱和理论模拟方法研究了可能杂质的结构。结果表明, 这种杂质是 TATB 分子的质子化合物, 命名为 1,3,5-三氨基-2,4,6-三硝基-2,5-环己二烯硫酸氢盐。依据量子化学方法, 这种杂质可能的形成机理是在溶解过程中, TATB 分子被浓硫酸中的 H 原子质子化。

关键词: 纳米 TATB; 杂质; 质子化合物; 机理

中图分类号: TJ55; O64

文献标志码: A

DOI: 10.11943/j.issn.1006-9941.2016.06.016